Geological Survey of Canada

Titles/Titres

Main page

Page principale

CURRENT RESEARCH

2004-A5

Geological setting of listwanite (carbonated serpentinite) at Atlin, British Columbia: implications for CO_2 sequestration and lode-gold mineralization

L.D. Hansen, R.G. Anderson, G.M. Dipple, and K. Nakano

2004

Natural Resources Canada Ressources naturelles Canada

Canada

ISSN 1701-4387
Catalogue No. M44-2004/A5E-PDF
ISBN 0-662-38618-3

Available in Canada from the
Geological Survey of Canada Bookstore website at:
http://gsc.nrcan.gc.ca/bookstore/ (Toll-free: 1-888-252-4301)

A copy of this publication is also available for reference by depository libraries across Canada through access to the Depository Services Program's website at http://dsp-psd.pwgsc.gc.ca

Authors' addresses

L.D. Hansen *(**lhansen@eos.ubc.ca**)*
G.M. Dipple *(**dipple@eos.ubc.ca**)*
K. Nakano *(**kfnakano@yahoo.ca**)*
Department of Earth and Ocean Sciences,
University of British Columbia,
Vancouver, British Columbia, V6T 1Z4

R.G. Anderson *(**boanders@nrcan.gc.ca**)*
Geological Survey of Canada,
2101-605 Robson Street,
Vancouver, British Columbia V6B 5J3

Publication approved by GSC Pacific, Vancouver

Original manuscript submitted: 2004-08-19
Final version approved for publication: 2004-10-18

Geological setting of listwanite (carbonated serpentinite) at Atlin, British Columbia: implications for CO_2 sequestration and lode-gold mineralization

L.D. Hansen, R.G. Anderson, G.M. Dipple, and K. Nakano

Hansen, L.D., Anderson, R.G., Dipple, G.M., and Nakano, K., 2004: Geological setting of listwanite (carbonated serpentinite) at Atlin, British Columbia: implications for CO_2 sequestration and lode-gold mineralization; Geological Survey of Canada, Current Research 2004-A5, 12 p.

Abstract: Carbonate-altered serpentinite (listwanite) is commonly associated with gold mineralization, but also binds large quantities of the greenhouse gas carbon dioxide. At Atlin, listwanite alteration progressed through three carbonation reactions that resulted in the same overall mineral transformations as proposed for the industrial sequestration of anthropogenic CO_2 by the process of mineral carbonation. Therefore, alteration of serpentinite to listwanite serves as a natural analogue to CO_2 sequestration. Listwanite alteration is concentrated along faults and two orthogonal fracture sets, and extends tens of metres into the wall rock. One fracture orientation is preferentially mineralized. The carbonation reactions most distal to the fracture system consume olivine and brucite, and record grain-scale percolation of CO_2-bearing fluids into serpentinite hundreds of metres from visible carbonate alteration. These previously unrecognized reactions may be relevant for in situ CO_2 sequestration. Extensive carbonation in the carbonate alteration systems generated fracture permeability that promoted further infiltration and may have accelerated carbonation and gold mineralization.

Résumé : La serpentinite altérée par carbonatation (listwanite), qui est souvent associée à la minéralisation en or, retient de grandes quantités de dioxyde de carbone, un gaz à effet de serre. Dans la région d'Atlin, l'altération en listwanite s'est faite par trois réactions successives de carbonatation, aboutissant aux mêmes transformations minérales que celles proposées pour la séquestration industrielle du CO_2 d'origine anthropique par un procédé de carbonatation des minéraux. L'altération de la serpentinite en listwanite agit donc comme un équivalent naturel de la séquestration du CO_2. L'altération en listwanite, concentrée le long de failles et de deux jeux orthogonaux de fractures, a pénétré jusqu'à des dizaines de mètres à l'intérieur de la roche encaissante. Les fractures de l'une des deux orientations ont été minéralisées de manière préférentielle. Les réactions de carbonatation qui ont eu lieu le plus loin du réseau de fractures ont consommé l'olivine et la brucite, témoignant que des fluides porteurs de CO_2 ont pénétré entre les grains de la serpentinite jusqu'à des centaines de mètres plus loin que la carbonatation visible. Ces réactions ignorées jusqu'à maintenant peuvent s'avérer pertinentes pour la séquestration in situ du CO_2. La carbonatation poussée du système a engendré des fractures, créant une perméabilité qui a par la suite facilité l'infiltration des fluides et pourrait avoir accéléré la carbonatation et la minéralisation en or.

INTRODUCTION

Listwanite forms from the reaction of ultramafic rocks with carbon dioxide–bearing fluid. This reaction is also a natural analogue to the geological sequestration of CO_2 by mineral carbonation. In mineral carbonation, CO_2 is chemically bound within carbonate minerals by the reaction of CO_2 with Mg^{2+} derived from serpentine and olivine. Globally, mineral carbonation offers virtually unlimited capacity and the promise of safe, permanent storage of CO_2 (Guthrie et al., 2001). In situ mineral carbonation, the direct injection of CO_2 into large subsurface ultramafic formations, allows for reaction times of tens to hundreds of years (Guthrie et al., 2001). Historically, listwanite is also known for its spatial association with lode-gold mineralization (e.g. Wittkopp, 1983; Schandl and Naldrett, 1992; Ash, 2001). Our goal in studying listwanite is to document reaction environments, pathways, catalysts, and reaction mechanics and uncover fluid-flow patterns and evidence for gold mobility. This information will aid in the development of in situ mineral carbonation systems and refine listwanite lode-gold deposit models.

Here we document the structural controls, mineral reactions, geochemical alteration, and permeability system which accompanied listwanite formation near Atlin, British Columbia (Fig. 1). Evidence for carbonation, indicated by Mg-carbonate minerals, is present for metres to tens of metres into wall rock adjacent to the fluid-controlling fractures. The results of 2003 field mapping and sampling show that listwanite occurs primarily along the basal décollement of an allochthonous ultramafic body and a transecting joint-and-fracture system. Listwanite alteration and serpentinization both effect magnetite stability. As a consequence, magnetic susceptibility was successfully tested as a tool to map the degree of serpentinization and carbonation reaction.

REGIONAL GEOLOGY AND FIELD METHODS

The ultramafic rocks at Atlin were first mapped by Aitken (1959) as ultramafic intrusions. Ash and Arksey (1990a) reinterpreted the rocks as the tectonically emplaced, residual upper mantle section of oceanic lithosphere. The ultramafic rocks, combined with associated oceanic rocks, including metabasalt and pelagic sedimentary rocks and mafic to ultramafic cumulates, form an assemblage of fault-bounded and dismembered, but geologically related, subunits. The Atlin Ophiolitic Assemblage (Ash and Arksey, 1990a) includes the ultramafic and mafic rocks, whereas the sedimentary accretionary rocks make up the Atlin Accretionary Complex (Ash and Arksey, 1990a). Both were obducted onto the Stikine and Cache Creek terranes during Early to Middle Jurassic amalgamation and accretion. This study focuses on the listwanite occurrences within the ultramafic section. Previous geological work around Atlin is described by Aitken (1959), Monger (1975, 1977a, b), Monger et al. (1978), Bloodgood et al. (1989), Mihalynuk et al. (1992), Ash and Arksey (1990a, b), Ash et al. (1991), and Ash (1994, 2001).

Figure 1. *Location of Atlin and the Atlin NTS 104N map area (yellow rectangles), northwestern British Columbia. Main rivers are shown in cyan and main highways in black.*

Geochemical studies of the Atlin listwanite include detailed petrography and geochemistry (Kellett, 2002; Hansen et al., 2003a, b, in press); mineralogical and geochemical studies of lode-gold prospects around the Atlin camp (Lueck, 1985; Newton, 1985); a fluid-inclusion study (Andrew, 1985); mineral chemistry of the principal minerals in the harzburgite (Ash, 1994); and ^{40}Ar-^{39}Ar and K-Ar geochronological ages of Cr-muscovite (Ash, 2001) interpreted as cooling ages related to Middle Jurassic batholiths.

Ash's map (1994) was the basis for choosing the study area and the foundation for the 1:6000 scale mapping of the listwanite within the Atlin Ultramafic Allochthon (Fig. 2). The nature and geometry of the structural zones were mapped at 1:20 scale from a well preserved listwanite zone on the west flank of Monarch Mountain (Fig. 3; Lowe and Anderson, 2002). All mapping was aided by an aeromagnetic map (Fig. 4), a magnetic susceptibility meter, and standard GPS techniques.

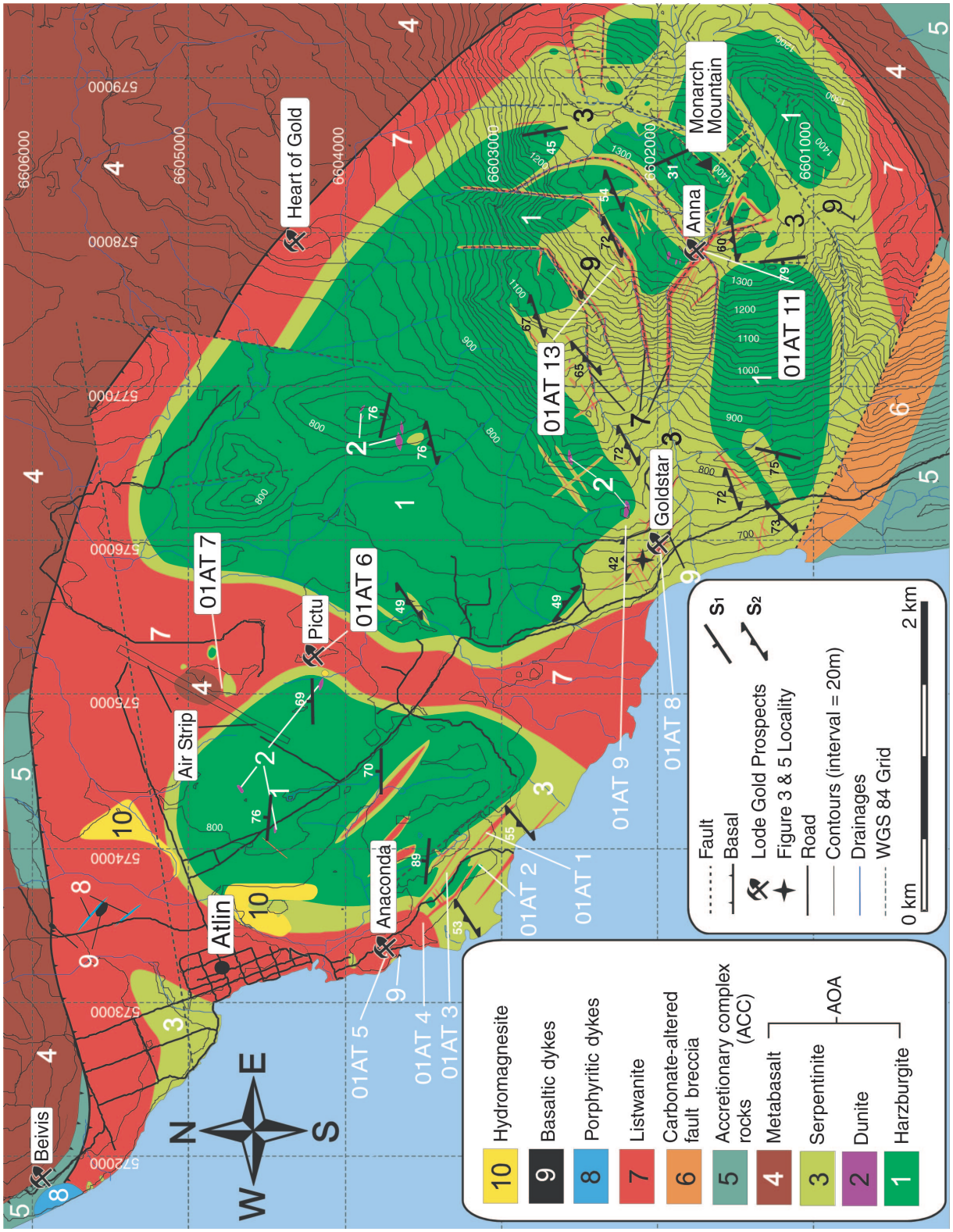

Figure 2. *Simplified geologic map of the study area showing the distribution of listwanite near Atlin area (this paper; Hansen et al., 2003b; Ash, 1994). AOA & AAC are Atlin Ophiolitic Assemblage and Atlin Accretionary Complex respectively of Ash & Arksey (1990a). Also shown are the Heart of Gold, Pictu, Anna, Anaconda, Beivis, and Goldstar gold prospects discussed in the text. Location of petrographic samples listed in Table 1 given by sample name (e.g. 01AT 5).*

ULTRAMAFIC ROCKS

The Atlin Ultramafic Allochthon (Ash and Arksey, 1990a), composed of serpentinized harzburgite, underlies an area of about 25 km^2 (Fig. 2) and comprises variably serpentinized, carbonitized, and deformed harzburgite with minor dunite lenses and pyroxenite veins. It is a tectonic klippe, separated from the Atlin Accretionary Complex rocks by a basal décollement termed the Monarch Mountain Thrust Fault (Ash and Arksey, 1990a). Serpentinization is most intensely developed near the basal décollement and adjacent to joints and fractures which crosscut the body (Fig. 2). The serpentine minerals are dominantly antigorite ± minor chrysotile that occur within fractures. The harzburgitic ultramafic rocks are divided into two units based on the degree of serpentinization.

The harzburgite unit includes all weakly to moderately serpentinized harzburgite (Fig. 5a, b). They are characteristically studded with 5 to 40 volume per cent resistant red-brown orthopyroxene grains (2–10 mm in diameter), often pseudomorphed by serpentine, within a recessive dun-brown-weathering, partially serpentinized olivine matrix. This unit forms rounded and jointed outcrops. Fresh surfaces are dark green, with the orthopyroxene crystals distinguished by their vitreous lustre and cleavage. Flattening of orthopyroxene grains defines a weakly to moderately developed, planar S_1 tectonite fabric (Fig 6a). Compositional layering is less common and defined by alternating 1 to 10 cm orthopyroxene-rich and -poor layers and is parallel to S_1. The freshest harzburgite is located at the west-central section on the plateau of Monarch Mountain where serpentine is <30 volume per cent (Fig. 5b).

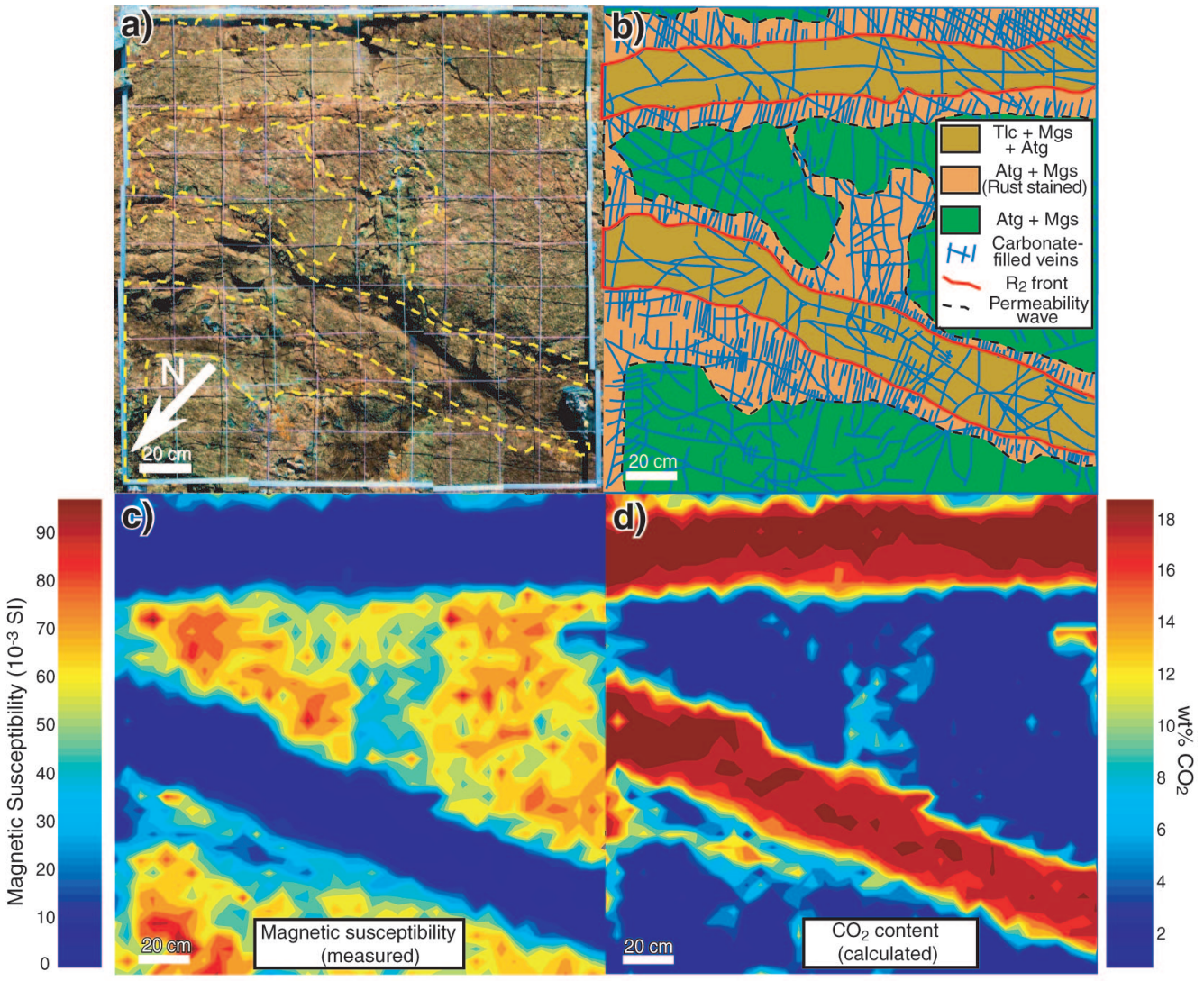

***Figure 3.**: **a)** Composite photograph of a 2 by 2 metre pavement outcropping on the western slope of Monarch Mountain (E 575887, N 6602098, NAD 83). **b)** Detailed geologic map of the listwanite zone mapped at 1:20 scale. **c)** Magnetic susceptibility map, composed of ca. 1550 measurements, showing the correlation of magnetic susceptibility with mineral content. **d)** Whole rock Wt% CO_2 map calculated from Hansen et al. (in press). The apparent small mis-correlation among contoured images and mapped geology is due to slightly different scales of each image. Abbreviations: Mgs – Magnesite, Atg – antigorite, Tlc – talc.*

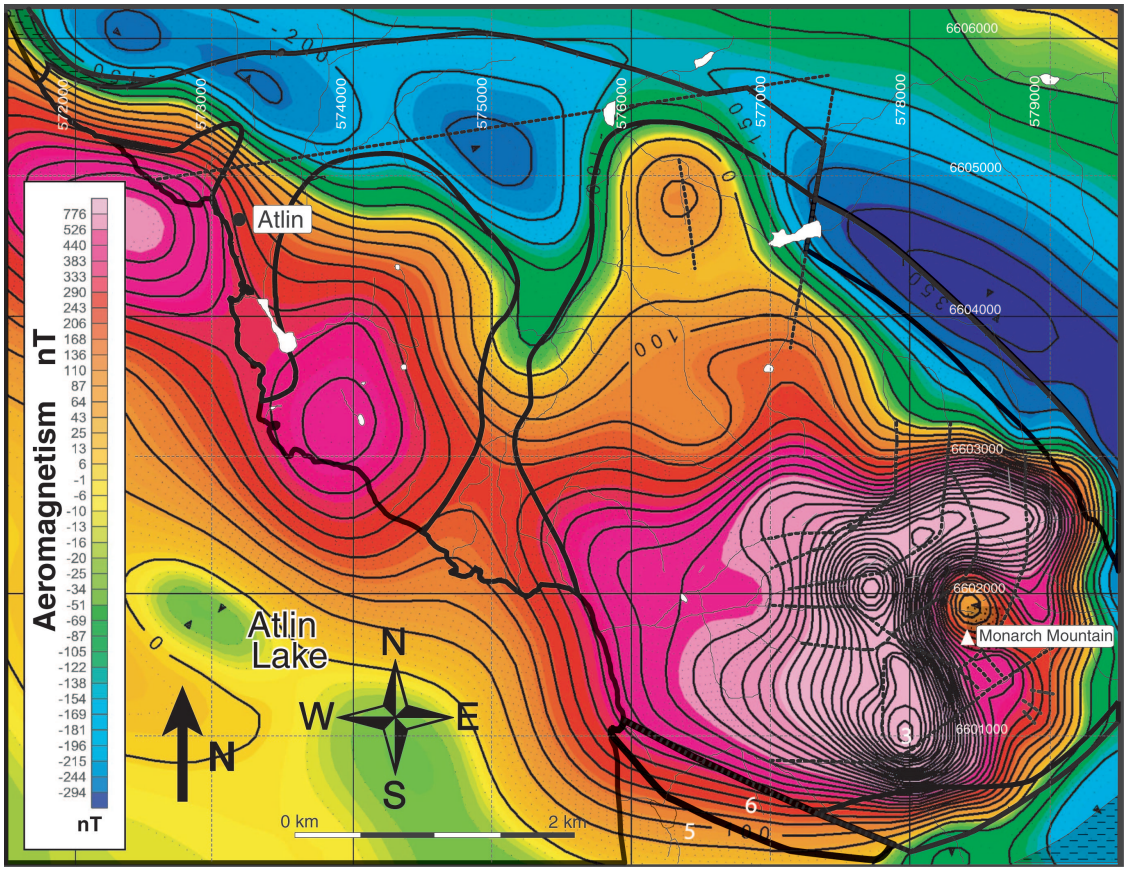

Figure 4. *Aeromagnetic map of the study area. Aeromagnetic lows correspond to known zones of listwanite. Aeromagnetic data from the National Geophysical Data Base maintained by the Geological Survey of Canada. Image generated by C. Lowe (GSC-Pacific).*

The serpentinite unit is intensely to completely serpentinized harzburgite (Fig. 5c, d). The contact is gradational, commonly making it difficult to differentiate the two units. The weathering colour of serpentinite is variable grey to near black, green, and blue. Lichen-free surfaces are spotted due to the presence of dark bastite after orthopyroxene. Commonly a well developed S_2 fabric, oriented 244º/54ºNW (Fig. 5c, 6b), is developed and defined by flattened and sheared bastite spots. Any relict orthopyroxene is mantled by bastite. The best examples of serpentinite occur along the lower west flank of Monarch Mountain, where the bastite foliation is common, and on the lakeshore north of Atlin where well polished rocks have a spotted green and dark blue texture.

Dunite lenses and pyroxenite veins, commonly too small to show in Figure 2, make up a small proportion of the map area. The lenses within the Atlin Ultramafic Allochthon range from less than 1 to about 100 m in length and form smooth 'dun' brown weathering outcrops. Dunite is commonly highly fractured, forming rubble within outcrops of more resistant harzburgite. The long axes of the lenses occur within the planar S_1 fabric of the harzburgite. Pyroxenite veins are generally 1 to 5 cm thick and generally are concordant with the S_1 foliation fabric. However, they are often isoclinally folded and often cut by later pyroxenite veins indicating they were emplaced pre- to post-deformation (Ash, 1994). The axial surfaces of the isoclinal folds parallel the tectonite fabric of the harzburgite.

The orientation of the S_2 fabric, as well as reported mullion structures (Ash and Arksey, 1990a) and southeasterly-southwesterly striking geological units to the south and to the east of the map area (Ash, 1994), suggest northwest-southeast shortening with "thrusting" to southeast (Ash and Arksey, 1990a). Interestingly, to the northwest, there is an area of geological units striking northwest-southeast. Listwanite-controlling faults and fractures are dominantly oriented parallel to these two directions.

LISTWANITE

Listwanite is a term used in Russian and Eastern European literature (e.g. Rose, 1837; Ploshko, 1963; Kashkai and Allakhverdiev, 1965; Halls and Zhao, 1995) to describe distinctive, rusty-red-weathering quartz-carbonate-chromium muscovite rocks produced during the carbonate alteration of ultramafic rocks. Listwanite and other mineral assemblages produced during the same carbonation process as listwanite are termed listwanite series assemblages and are akin to the rocks of this study (Fig. 7). In North America, listwanite is

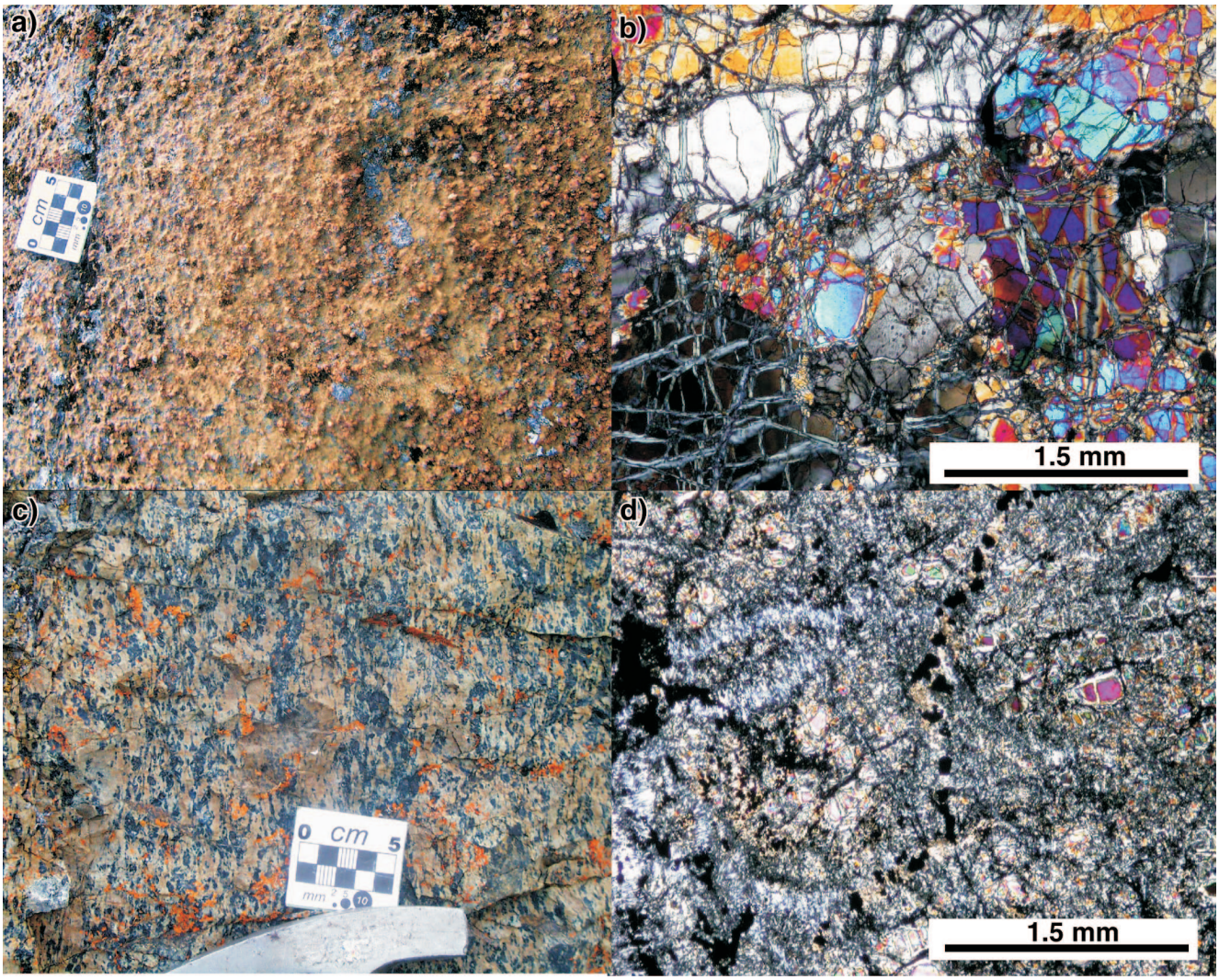

Figure 5. ***a)*** *Resistant orthopyroxene within recessive, partially serpentinized olivine matrix; typical of weakly serpentinized harzburgite.* ***b)*** *Photomicrograph of freshest harzburgite under cross-polars.* ***c)*** *Moderately foliated serpentinite defined by the flattening of bastite spots.* ***d)*** *Photomicrograph of typical serpentinite under cross-polars.*

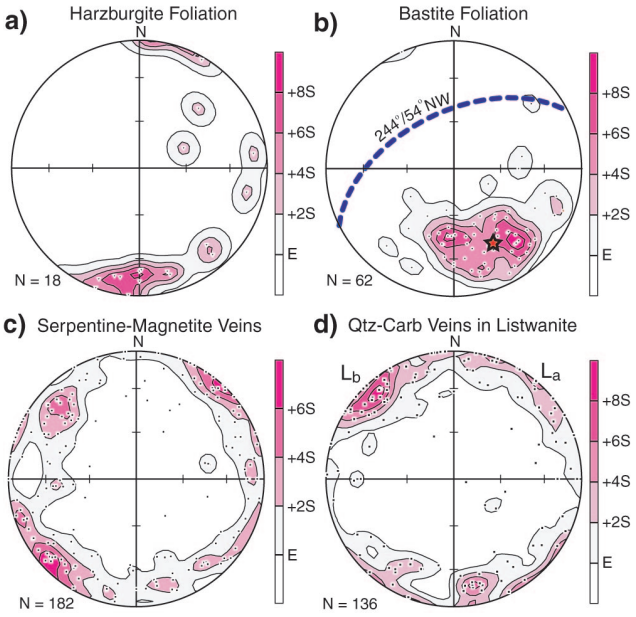

Figure 6.

Structural data (poles to planes on equal area stereonets) of: ***a)*** *Harzburgite foliation defined by flattening of orthopyroxene grains;* ***b)*** *Bastite foliation defined by flattened and sheared bastite spots;* ***c)*** *Magnetite-serpentine veinlets; d) quartz-carbonate veins associated with high-grade listwanite.*

more broadly defined as; "a carbonitized and variably silicified serpentinite, occurring as dykes in ophiolite complexes" (Jackson, 1997). Unfortunately this definition is inappropriate for use at Atlin because it implies metasomatism, which has been discounted at Atlin (Hansen et al., 2003a, b, in press). Furthermore, listwanite alteration is a multistep process (Hansen et al. in press) and intermediate mineral assemblages do not contain quartz (Table 1). The other common North American term 'silica carbonate alteration', used to describe these deposits, is also not suitable for the same reasons. Consequently, our usage of listwanite refers to any carbonate-altered serpentinite. Halls and Zhao (1995) discuss listwanite terminology in greater detail.

At Atlin, listwanite occurs along the shallowly dipping lower boundary of the Atlin Ultramafic Allochthon (Fig. 2 and 7b). Any brecciation appears to predate listwanite alteration. Listwanite also is common along steeply dipping faults and fractures dominantly trending about 140° (L_a trend) and 50° (L_b trend) (Fig. 2, 6d, 7a). South of Atlin, the L_b trend consistently cuts the L_a-trending zones, possibly recording multiple listwanite-generation events. Fracture-controlled listwanite is generally expressed as lineament depressions, commonly vegetated and filled with overburden. Rusty-red-weathering side walls confirm they are underlain by listwanite. The lineament and listwanite association is clearly seen at the head of the Monarch Mountain hiking trail on Warm Bay road (Fig. 8).

Within the harzburgite unit, the margins of surface lineaments are commonly marked by chalky blue-green-weathering serpentine alteration, suggesting that they mark structural weaknesses which acted to focus fluids. The serpentinization along fractures is overprinted by listwanite. Small serpentine-magnetite veinlets, usually less than 1 cm thick, cut harzburgite, dunite, and serpentinite. Structural measurements indicate that the dominant orientations of the veinlets are collinear with lineament and listwanite trends (Fig. 6c, d).

Generally, L_a listwanite zones are fewer but commonly more extensive, pervasively carbonated, and contain more stockwork quartz-carbonate veins and Cr-muscovite than L_b zones. The highest concentration of L_a zones transects the map area, extending from about 700 m south of Atlin to the west side of Monarch Mountain, about 3 km southeast of town (Fig. 2). It may mark the locus of a broad fault or fracture zone. The Anna and Goldstar gold prospects, the only showings in the map area clearly not associated with the basal décollement, are both associated with L_a-trending listwanite zones and Cr-muscovite.

LISTWANITE PETROGRAPHY, GEOCHEMISTRY AND REACTION PATH

Listwanite at Atlin is zoned mineralogically outward from the controlling fracture permeability network and tracks the migration of three nonmetasomatic carbonation-(de)hydration reactions (Hansen et al., in press). The most distal reaction (R_1) was detected geochemically and petrographically (Table 1) and involves the breakdown of olivine ± brucite (assemblage A_1, Fig. 9) to magnesite plus antigorite (A_2). The magnesite-antigorite rocks often resemble serpentinite (A_1) but, in outcrop, commonly contain small carbonate

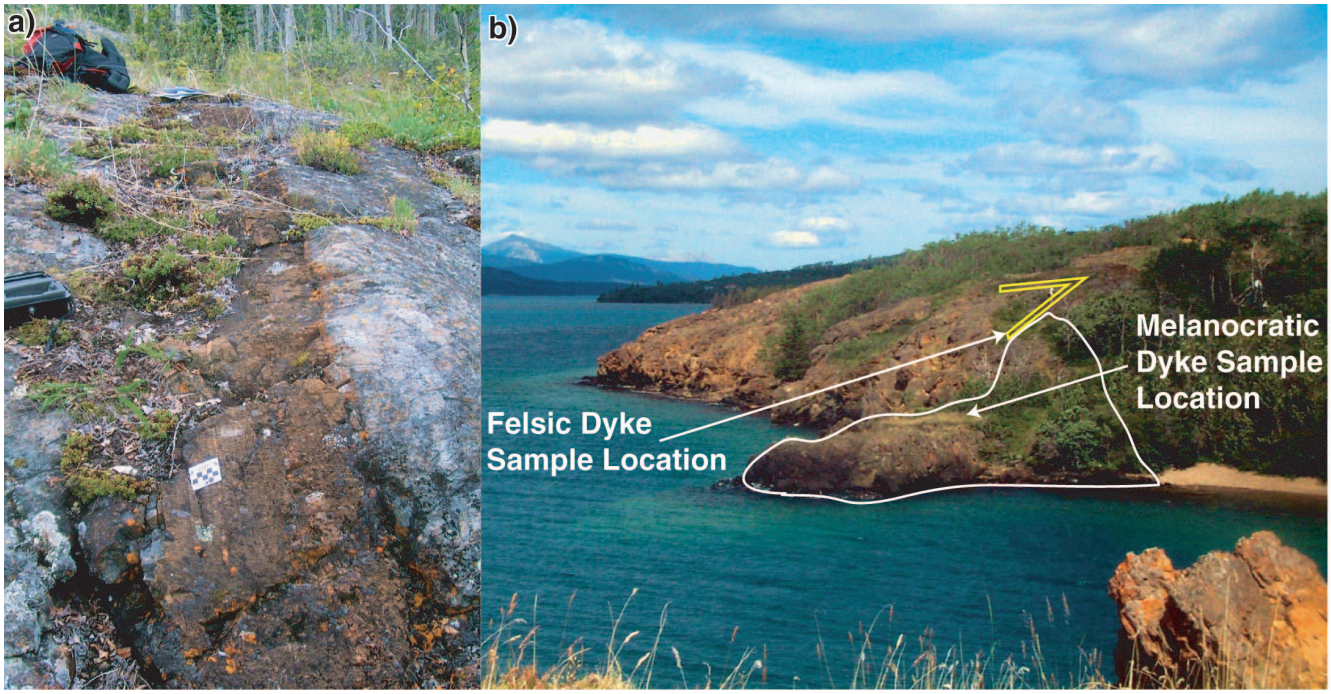

Figure 7.a) *View to northwest to well-preserved, rusty-brown, talc-magnesite listwanite zone (L_b) which is about 50 cm thick. Scale = 5cm.* ***b)*** *View to the north to a large area of distinctive rusty red listwanite associated with the basal décollement (below water) along eastern shore of Atlin Lake. The small peninsula in the centre of the image is underlain by a melanocratic basaltic dyke.*

Table 1. Mineralogy of carbonated serpentinite from Atlin, British Columbia.

Sample	Chr	Mgt	Brc	Ol	Atg	Mgs	Tlc	Qtz		CO_2 (wt%)
01AT-8-1	x	x			x				A_1	0.06
01AT-13-1	x	x			x				A_1	0.10
01AT-3-1	x	x	x		x				A_1	0.21
01AT-10-1	x	x	x	x	x				A_1	0.15
01AT-10-2	x	x	x	x	x	x[v]			A_1	0.26
01AT-2-2	x	x	x	x	x				A_1	0.33
01AT-9-1	x	x		x	x	x			R_1	2.10
01AT-11-1	x	x		x	x	x			R_1	2.57
01AT-1-9	x	x			x	x			A_2	3.37
01AT-6-3	x	x			x	x			A_2	4.00
01AT-1-8	x	x			x	x			A_2	4.60
01AT-13-2	x	x			x	x			A_2	7.12
01AT-11-2	x	x			x	x			A_2	9.60
01AT-7-3	x	x			x	x	x		R_2	3.40
01AT-1-7	x	x			x	x	x		R_2	7.19
01AT-1-6	x	x			x	x	x		R_2	9.54
01AT-9-2	x				x	x	x		R_2	17.26
01AT-7-1	x					x	x	x	R_3	21.83
01AT-5-4	x	x[y]				x	x	x	R_3	28.01
01AT-1-5	x	x[z]			x[w]	x	x	x	R_3	34.00
01AT-4-1	x					x	x	x	R_3	34.34
01AT-5-2	x					x		x	A_4	35.20
01AT-6-1*	x					x		x	A_4	36.19

[v] Only occurs in small veins
[w] Occurs in small isolated patches
[y] Armoured relics & late mantling of chromite and pyrite
[z] Magnetite in late fractures & late mantling of chromite
* Sample contains Cr-muscovite
Abbreviations: A – assemblage number, Atg – antigorite, Brc – brucite, Chr – chromite, Mgs – magnesite, Mgt – magnetite, Ol – olivine, Qtz –quartz, R – reaction number, Tlc – talc, and x – mineral present.

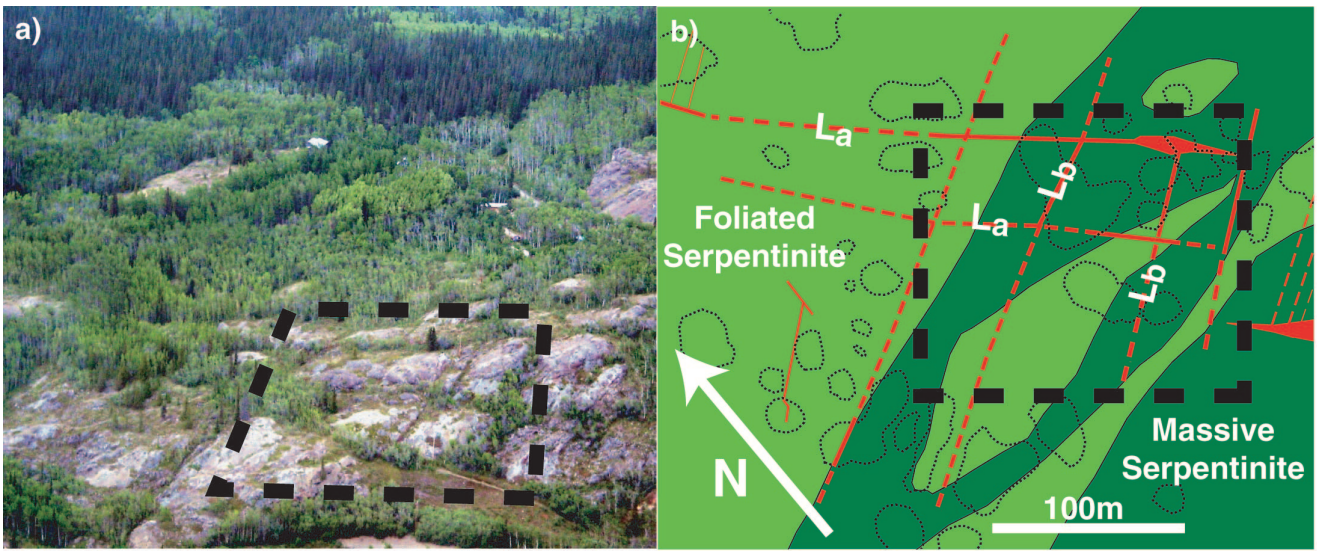

Figure 8. a) *Aerial view to the northeast showing recessive weathering lineaments representing L_a and L_b orientations associated with listwanite at head of Monarch Mountain Hiking trail (photo by M. Mihalynuk, August 2003) (E 575900, N 6602100, NAD 83).* ***b)*** *Geologic map of the area pictured in Fig. 4a.*

veinlets. The low abundance of olivine in serpentinite (A_1) limits reaction R_1. Antigorite-magnesite grades into talc-magnesite (A_3) produced via reaction R_2. It is soft, has a waxy feel and often weathers to a distinctive smooth but irregular dark-red surface. Quartz plus magnesite (A_4) is present in completely carbonated areas which resulted from the carbonation of talc (R_3). The quartz-magnesite zone weathers to a rough orange-red surface. Minor chromite present in serpentinite survives all three reactions.

$$34\ Mg_2SiO_4 + 20\ CO_2 + 31\ H_2O \rightarrow Mg_{48}Si_{34}O_{85}(OH)_{62} + 20\ MgCO_3 \quad \mathbf{(R_1)}$$

Olivine → Antigorite + Magnesite

$$2\ Mg_{48}Si_{34}O_{85}(OH)_{62} + 45\ CO_2 \rightarrow 45\ MgCO_3 + 17\ Mg_3Si_4O_{10}(OH)_2 + 45\ H_2O \quad \mathbf{(R_2)}$$

Antigorite → Magnesite + Talc

$$Mg_3Si4O_{10}(OH)_2 + 3\ CO_2 \rightarrow 3\ MgCO_3 + 4\ SiO_2 + H_2O \quad \mathbf{(R_3)}$$

Talc → Magnesite + Quartz

Olivine is not present with talc, and quartz does not occur with serpentine, indicating that the three reactions have occurred in sequence. The mineral zonation is therefore amenable the mapping of metamorphic isograds: the magnesite, talc, and quartz isograds indicate the first appearance of magnesite, talc, and quartz, respectively. Highly altered cores may contain stockwork quartz-carbonate veins, bright green Cr-muscovite (mariposite, fuchsite), sulphide mineralization (mainly pyrite), and anomalous Au values. Occurrence of Cr-muscovite results from limited chromite destruction and the addition of K^+. Though Ca^{2+} addition is common in listwanite systems (e.g. Aydal, 1990), to date the authors' studies have been unable to detect it at Atlin.

IGNEOUS INTRUSIONS

At least two distinct phases of dykes are present in the map area. The first is a melanocratic medium-grained plagioclase-hornblende gabbro. The other is a medium- to coarse-grained feldspar-, quartz, and biotite-porphyry dyke phase with a light-grey aphanitic groundmass. Both contain sulfide minerals, mostly pyrite. Locally both are carbonated, but most clearly crosscut the listwanite. This crosscutting relation is clearly seen about 500 m south of Atlin near the Anaconda lode-gold prospect (Fig. 6b). Xenoliths of listwanite occur within the mafic dyke phase at this location. Dykes are commonly spatially associated with listwanite and surface lineaments. Regional crustal weaknesses may have provided the same guides to magma ascent as they did for fluids associated with earlier episodes of serpentinization and listwanite generation. Two U-Pb geochronological analyses of unaltered dykes, one from each phase which crosscuts listwanite, and a fresh ^{40}Ar-^{39}Ar geochronological biotite sample from a dyke which shows evidence of carbonate alteration are in progress. These studies will further constrain the age and duration of the listwanite genesis at Atlin and may show a temporal correlation with the widespread Middle Jurassic plutonism in the area, a potential source of gold-rich fluid.

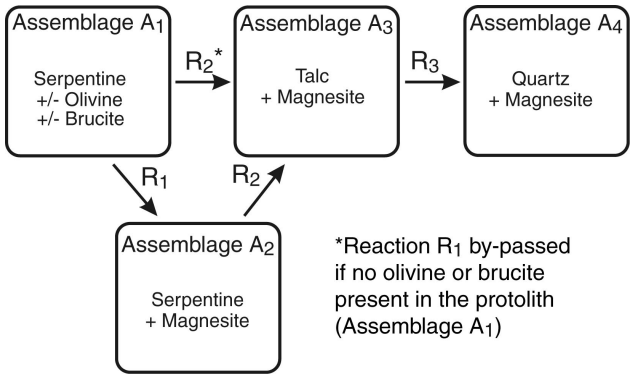

Figure 9. *Simplified flow chart for the reaction path of the Atlin listwanite system during progressive carbonation of serpentinite. Detailed description in Hansen et al. (2004).*

MAGNETISM

Magnetite forms during the serpentinization of olivine and is destroyed during carbonate alteration. During serpentinization, iron contained in harzburgitic (Fo_{90}) olivine is preferentially excluded from serpentine, resulting in the formation of magnetite (Toft et al., 1990). Magnetite occurs as rim overgrowths on chromite and as disseminated grains aligned in foliation planes and in fractures. All increase the magnetic susceptibility of the serpentinite rocks. Magnetic susceptibility varies strongly between the harzburgite unit (2 to 50 (10^{-3} SI units)) and serpentinite unit (>50 to as high as 150 (10^{-3} SI units)). This observation is useful for differentiating between the two units in lichen-covered areas where the degree of serpentinization is not easily discernable.

Magnetite is progressively consumed during reaction R_2 (Hansen et al., in press). The Fe derived from the breakdown of magnetite was accommodated in magnesite. Magnetic susceptibility values are usually close to the detection limit of the KT-9 Kappameter hand-held magnetic susceptibility meter ($1x10^{-5}$ SI units) in rock containing > 20 wt% CO_2, corresponding to complete progress of reaction R_2. A magnetic-susceptibility contour map, including approximately 1550 magnetic-susceptibility measurements from the detailed mapping area of a L_b listwanite zone, illustrates the association of magnetic susceptibility with mineralogy (Fig. 3c). Following Hansen et al. (in press), a CO_2 content map was calculated from the magnetic susceptibility map (Fig. 3d) and tracks whole-rock CO_2 content to within 5 wt %.

Airborne magnetic surveys are able to detect areas of vast carbonate alteration (e.g. Ash, 1994; Lowe and Anderson, 2002). Areas of listwanite alteration shown in Figure 2 correspond to aeromagnetic lows shown in Figure 4. The basal décollement that traces from just north of Atlin to the Heart of Gold prospect, then along the east to south slopes of Monarch Mountain is easily distinguished on the aeromagnetic map

(Fig. 2, 4). The aeromagnetic saddles in Figure 4 through and just south of Atlin, and through the Pictu prospect, correspond to areas of known listwanite.

IMPLICATIONS FOR CO_2 SEQUESTRATION

The overall mineral transformation in listwanite alteration is the same as that proposed for sequestration of CO_2 in minerals, but in nature proceeds through a series of sub-reactions preserved as spatially distinct zones. Direct carbonation of olivine ± brucite (R_1) was previously unrecognized at Atlin, and records carbonation of intact bedrock many tens of metres from the primary fracture permeability system. Initial carbonation of olivine by reaction R_1 is likely due to the higher reactivity of olivine (± brucite) than that of serpentine in the presence of a CO_2-bearing fluid (Lackner et al., 1995; Guthrie et al., 2001) and the small solid-volume increase associated with the carbonation of small amounts of relict olivine (Table 2). Though reaction R_1 only accounts for about 5 to15 % the carbonation potential for the serpentinite at Atlin (Table 1), because it is widespread, it may have sequestered a significant portion of the total CO_2 contained in the Atlin listwanite system.

Each of the three carbonation reactions involves an increase in the volume of solids, therefore each has the potential to create or destroy permeability. Reaction R_2 binds large quantities of CO_2 with small associated loss of porosity and permeability (Table 1, 2). Moreover, the progression of the reaction R_2 may create a permeability front in advance of it, promoting further carbonation. The development of carbonate veins orthogonal to the R_2 reaction front in Figures 3a and b may represent fracture permeability generated in tension (Hansen et al., in press). The mechanical model of Jamtveit et al. (2000) predicted the development of high permeability zones downstream of an advancing reaction undergoing a solid-volume increase. Indeed, the pattern of reaction and vein formation in Figures 3a and b resembles the model prediction. The distribution of tensile fractures approximately marks the outer extent of rust-weathering serpentinite, suggesting they have enhanced percolation of reactive CO_2-bearing fluid into the wall rock.

Complete carbonation to magnesite plus quartz (A_4) is generally limited to the cores of the largest systems. The large solid-volume gain associated with reaction R_3 may seal the fluid percolation pathways and limit the usefulness of in situ mineral carbonation systems. For this reason, reactions R_1 and R_2, that combined account for about half of the carbonation potential for serpentinite (Table 1), may hold the most promise for in situ carbonation of minerals. The stability of the three reaction steps is controlled by the activity of CO_2 in the fluid phase (Hansen et al., in press). Therefore, industrial mineral carbonation systems could potentially be tailored to drive only those reactions favourable for carbonating bedrock.

Table 2. Volume changes.

Reaction	ΔVs* (rxn)	ΔVs (rock**)
R_1: Ol → Atg + Mgs	55.1%	4.2%
R_2: Atg → Talc + Mgs	2.6%	2.3%
R_3: Tlc → Qtz + Mgs	28.5%	16.2%

* Calculated from Berman (1988) at 250°C and 500 bars
** Assuming 7.5% relict olivine by vol.
Abbreviations: Atg – antigorite, Mgs – magnesite, Ol – olivine, Qtz – quartz, R – reaction number, Tlc – talc, ΔVs*(rock) – solid volume change for the rock, and ΔVs*(rxn) – solid volume change for the reaction.

IMPLICATIONS FOR LODE-GOLD MINERALIZATION

A positive correlation of Au with potassium-altered quartz-carbonate listwanite has been noted in listwanite systems worldwide (e.g. Ploshko, 1963; Buisson and LeBlanc, 1987; Ash and Arksey, 1991). Ploshko (1963) also noted an association of potassium alteration in listwanite systems with felsic igneous intrusions in the northern Caucasus. Similarly, Ash (2001) noted a general correlation in ophiolite-hosted Au occurrences with granitic intrusions in the Canadian Cordillera. Granitic intrusions could promote listwanite development by providing a heat source to drive fluid circulation, and by serving as a fluid source, and possibly as a source for gold and other metals.

Middle Jurassic plutonism is widespread to the south and immediately north of the listwanite occurrences. Southern plutons include the Mount McMaster and Llangorse Mountain batholiths (172 ± 0.3 Ma and 171 ± 0.3 Ma (U-Pb), respectively (Anderson et al., 2003)) 45 to 60 km south of Atlin. The south margin of the large, multiphase Middle Jurassic Fourth of July batholith occurs a few kilometres to the north of the Atlin Ultramafic Allochthon. The batholith's U-Pb zircon age range of 166 to 174 Ma (Mihalynuk et al., 1992) completely overlaps the age range of Cr-muscovite in the listwanite (168–172 Ma (^{40}Ar-^{39}Ar); Ash, 2001). Streams that drain the Fourth of July batholith contain stream sediments with anomalous Au contents (Jackaman, 2000), suggesting the intrusion was a possible source for Au and other metals. A small stock correlated with the Fourth of July batholith outcrops between Monarch Mountain and Union Mountain (Ash, 1994), suggesting thermal influence of the batholith in the study area. As well, new isotopic ages for dykes in the study area may show a direct correlation to the Middle Jurassic plutonism. Magmatic-hydrothermal activity associated with the Fourth of July batholith may have contributed to gold mineralization in the Atlin area.

Lode-gold prospects near Atlin are spatially associated with the most intense Cr-muscovite-bearing listwanite zones along the basal décollement and in the L_a orientation. L_a listwanite zones therefore may be preferential targets for future exploration. Listwanite alteration destroys magnetite. Zones of listwanite appear as magnetic lows on aeromagnetic survey maps (Fig. 4). Ground surveying with a magnetic susceptibility meter could help identify subtle to cryptic carbonation which may aid in vectoring to potential lode-gold deposits.

ACKNOWLEDGMENTS

This research was funded by a Natural Sciences and Engineering Council of Canada Discovery Grant, by the Oil, Gas and Energy Branch of Environment Canada, and by the Innovative Research Initiative for Greenhouse Gas Mitigation, a program under the Climate Change Action Plan 2000, and administered under Environment Canada and Natural Resources Canada, Earth Sciences Sector. It was conducted under the auspices of Activity 5.3a, "CO_2 Storage by Mineral Carbonation Reactions: Kinetic and Mechanical Insights from Natural Analogues" under the Earth Sciences Sector Climate Change Program, Project CC4500, entitled "Monitoring methods and assessment of carbon sequestration over Canada's landmass".

We thank Bill Reynen, Environment Canada, for encouraging the initiation of this project and Mitch Mihalynuk, British Columbia Geological Survey Branch, for his help and expertise at Atlin, including logistics, data sharing, and aerial photography. Carmel Lowe introduced us to the utility of magnetic susceptibility as a mapping tool. We have benefited from many discussions on and off outcrop with Terry Gordon of the University of Calgary.

REFERENCES

Aitken, J.D.
1959: Atlin map area, British Columbia; Geological Survey of Canada, Memoir 307, 89 p.

Anderson, R.G., Lowe, C., and Villeneuve, M.E.
2003: Nature, age, setting, and mineral potential of some Mesozoic plutons in central and northwestern Atlin map area (NTS 104 N), northwestern B.C.; Geological Association of Canada–Mineralogical Association of Canada–Society of Economic Geologists, Annual General Meeting, Vancouver 2003 Abstracts, v. 28, abstract no. 600, CD-ROM.

Andrew, K.
1985: Fluid inclusion and chemical studies of gold-quartz veins in the Atlin camp, northwestern British Columbia; B.Sc. thesis, University of British Columbia, Vancouver, British Columbia, 116 p.

Ash, C.H.
1994: Origin and tectonic setting of ophiolitic ultramafic and related rocks in the Atlin area, British Columbia (NTS 104 N); British Columbia Ministry of Energy, Mines and Petroleum Resources, Bulletin 94, 48 p.
2001: Relationship between ophiolites and gold-quartz veins in the North American Cordillera; British Columbia Department of Energy, Mines and Petroleum Resources, Bulletin 108, 140 p.

Ash, C.H. and Arksey, R.L.
1990a: The Atlin Ultramafic Allochthon: ophiolite basement within the Cache Creek Terrane; tectonic and metallogenic significance (104 N/12); Geological Fieldwork 1989, British Columbia Department of Energy and Mines, Paper 1990-1, p. 365–374.
1990b: The listwanite-lode gold association in British Columbia; Geological Fieldwork 1989, British Columbia Department of Energy and Mines, Paper 1990-1, p. 359–364.

Ash, C.H., Macdonald, R.W. J. and Arksey, R.L.
1991: Towards a deposit model for ophiolite related mesothermal gold in British Columbia; Geological Fieldwork 1991, British Columbia Department of Energy and Mines, Paper 1992-1, p. 253–260.

Aydal, D.
1990: Gold-bearing listwaenites in the Arag Massif, Kastamonu, Turkey; Terra Nova, v. 2, p. 43–52.

Berman, R.G.
1988: Internally-consistent thermodynamic data for minerals in the system: Na_2O-K_2O-CaO-FeO-Al_2O_3-SiO_2-TiO_2-H_2O-CO_2; Journal of Petrology, v. 29, pt. 2, p. 445–522.

Bloodgood, M.A., Rees, C.J., and Lefebure, D.V.
1989: Geology and mineralization of the Atlin area, northwestern British Columbia (104 N/11W and 12E); Geological Fieldwork 1988, British Columbia Department of Energy and Mines Paper 1989-1, p. 311–322.

Buisson, G. and LeBlanc, M.
1987: Gold in mantle peridotites from Upper Proterozoic ophiolites in Arabia, Mali, and Morocco; Economic Geology, v. 82, p. 2091–2097.

Guthrie, G.D., Carey, J.W., Bergfeld, D., Byer, D., Chipera, S., Ziock, H., and Lackner, K.S.
2001: Geochemical aspects of the carbonation of magnesium silicates in an aqueous medium; Proceedings of the First National Conference on Carbon Sequestration, National Energy Technology Laboratory, May 14–17, 2001, Washington, D.C., session 6C, 14 p.

Halls, C. and Zhao, R.
1995: Listvenite and related rocks: perspectives on terminology and mineralogy with reference to an occurrence at Cregganbaun, County Mayo, Republic of Ireland; Mineralium Deposita, v. 30, p. 303–313.

Hansen, L.D., Dipple, G.M., and Anderson, R.G.
2003a: Carbonate altered serpentinites of Atlin, BC: a two stepped analog to CO_2 sequestration; Geological Society of America, 2003 annual meeting, Seattle, WA; Abstracts with Programs - Geological Society of America; Session 144-14.

Hansen, L. D., Dipple, G. M., and Gordon, T. M.
2003b: Carbonate-altered serpentinites, Atlin, BC: a natural analog to CO_2 sequestration; Geological Association of Canada–Mineralogical Association of Canada–Society of Economic Geologists, Annual General Meeting, Vancouver 2003, Abstracts, v. 28, abstract no. 494, CD-ROM.

Hansen, L.D., Dipple, G.M., Kellett, D.A., and Gordon, T.M.
in press: Carbonate-altered serpentinite: a geologic analog to carbon dioxide sequestration, Canadian Mineralogist.

Jackaman, W.
2000: British Columbia Regional Geochemical Survey – Atlin (NTS 104 N). Stream sediment and water geochemical data and map booklet; British Columbia Ministry of Energy, Mines and Petroleum Resources, RGS 51, 173 p.

Jackson, J.A.
1997: Glossary of Geology, American Geological Institute, Alexandria, Virginia, 769 p., (fourth edition).

Jamtveit, B., Austrheim, H., and Malthe-Søenssen, A.
2000: Accelerated hydration of the Earth's deep crust induced by stress perturbations; Nature, v. 408, p. 75–87.

Kashkai, A.M. and Allakhverdiev, I.
1965: Listwanites: their origin and classification; United States Geological Survey, Library, Reston, Virginia, United States, 146 p., Translated from the Russian, Listvenity, ikh genezis i klassifikatsiya; Izvestiya Akademii Nauk Azerbajdzhanskoj SSR. Seriya Fiziko-Tekhnicheskikh i Matematicheskikh Nauk. Izdatel'stvo Ehlm, Baku, 1965.

Kellett, D.A.
2002: Geochemical and geophysical monitors of reaction progress during carbonate alteration of serpentinite at Atlin, British Columbia; B.Sc. thesis, University of British Columbia, Vancouver, British Columbia, Canada, 48 p.

Lackner, K.S., Wendt, C.H., Butt, D.P., Joyce, E.L., and Sharp, D.H.
1995: Carbon dioxide disposal in carbonate minerals; Energy, v. 20, 1153–1170.

Lowe, C. and Anderson, R.G.
2002: Preliminary interpretations of new aeromagnetic data for the Atlin map area, British Columbia; Geological Survey of Canada, Current Research 2002-A17, 11 p.

Lueck, B.A.
1985: Geology of carbonitized fault zones on the Anna claims and their relationship to gold deposits, Atlin, British Columbia; B.Sc. thesis, University of British Columbia, Vancouver, British Columbia, Canada, 55 p.

Mihalynuk, M.G., Smith, M., Gabites, J.E., Runkle, D., and Lefebure, D.
1992: Age of emplacement and basement character of the Cache Creek terrane as constrained by new isotopic and geochemical data; Canadian Journal of Earth Sciences, v. 29, p. 2463–2477.

Monger, J.W.H.
1975: Upper Paleozoic rocks of the Atlin terrane; Geological Survey of Canada, Paper 74-47, 63 p.
1977a: Upper Paleozoic rocks of northwestern British Columbia; *in* Current Research, Part A, Geological Survey of Canada, Paper 77-1A, p. 255–262.
1977b: Upper Paleozoic rocks of the western Canadian Cordillera and their bearing on the Cordilleran evolution; Canadian Journal of Earth Sciences, v. 14, p. 1832–1859.
Monger, J.W.H., Richards, T.A., and Paterson, I.A.
1978: The hinterland belt of the Canadian Cordillera: new data from northern and central British Columbia; Canadian Journal of Earth Sciences, v. 15, p. 823–830.
Newton, D.
1985: A study of carbonate alteration of serpentinites around Au and Ag bearing quartz veins in the Atlin camp, British Columbia; B.Sc. thesis, University of British Columbia, Vancouver, British Columbia, Canada, 85 p.
Ploshko, V.V.
1963: Listwaenitization and carbonitization at terminal stages of Urushten igneous complex, North Caucasus; International Geology Review, v. 7, p. 446–463.
Rose, G.
1837: Mineralogisch-geognostistiche Reise nach dem Ural, dem Altai und dem Kaspischen Meere. v. 1: Reise nach dem nordlichen Ural und dem Alta; C.W. Eichoff (Verlag der Sanderschen Buchhandlung), Berlin, Germany, 641 p.
Schandl, E.S. and Naldrett, A.J.
1992: CO_2 metasomatism of serpentinites, south of Timmins, Ontario; Canadian Mineralogist, v. 30, p. 93–108.
Toft, P.B., Arkani-Hamed, J., and Haggerty, S.E.
1990: The effects of serpentinization on density and magnetic susceptibility: a petrophysical model; Physics of the Earth and Planetary Interiors, v. 65, p. 137–157.
Wittkopp, R.W.
1983: Hypothesis for the localization of gold in quartz veins, Allegheny district; California Geology, p. 123–127.